Ingeniería y Ciencia
ISSN:1794-9165 | ISSN-e: 2256-4314
ing. cienc., vol. 12, no. 23, pp. 11–23, enero-junio. 2016.
http://www.eafit.edu.co/ingciencia

Influence of Si Atoms Insertion on the Formation of the Ti-Si-N Composite by DFT Simulation

Juan Manuel González [1], Johans Steeven Restrepo [2], Carolina Ortega Portilla [3]
Alexander Ruden Muñoz [4]and Federico Sequeda Osorio [5]

Received: 08-10-2015 | Accepted: 21-01-2016 | Online: 01-02-2016

PACS:31.15.xr

doi:10.17230/ingciencia.12.23.1

Abstract

Using Density Functional Theory (DFT) SiN and TiN structures were simulated, in order to study the influence of the silicon atoms insertion in the TiN lattice placed on interstitial and substitutional positions in a face centered cubic (FCC) crystalline lattice. Results showed that the $SiN - FCC$ structure is pseudo-stable; meanwhile the tetragonal structure is stable with ceramic behavior. The $TiN - FCC$ structure is stable with ceramic behavior similar to $SiN - Tetragonal$. 21% silicon atoms insertion in interstitial positions showed high induced deformation, high polarization and $Si - N$ bond formation, indication an amorphous transition that could lead to the production of a material composed from TiN grains or nano-grains embedded in a $Si - N$ amorphous matrix. When

[1] Universidad del Valle, Cali, Colombia, Juan.gonzalez@correounivalle.edu.co.
[2] Universidad Nacional Autónoma de México, Ciudad de México, México, johansrestrepo@hotmail.com.
[3] Universidad del Valle, Cali, Colombia, carolinaortega35@gmail.com.
[4] Universidad Tecnológica de Pereira, Pereira, Colombia, arudenm@gmail.com.
[5] Universidad del Valle, Cali, Colombia, Federico.sequeda@correounivalle.edu.co.

including 21% of silicon atoms, substituting titanium atoms, the distribution showed higher stability that could lead to the formation of different phases of the stoichiometric $Ti_1 -_x Si_x N_y$ compound.

Key words: density functional theory; crystalline structure; nano-composite; silicon; thin films; coatings.

Influencia de la inserción de átomos de Si en la formación del compuesto Ti-Si-N por simulación DFT

Resumen

Se simularon estructuras del SiN y TiN utilizando Teoría de Funcionales de Densidad (DFT), con el fin de estudiar la influencia de la inserción de átomos de Si en la estructura del TiN en posiciones intersticiales y sustitucionales de una red cristalina cúbica centrada en las caras (FCC). Los resultados mostraron que la estructura SiN-FCC es pseudo estable, mientras que la estructura tetragonal es estable, con comportamiento cerámico. La estructura del TiN-FCC es estable con un comportamiento cerámico similar al del SiN-tetragonal. La inserción de 21 % de átomos de Si en posiciones intersticiales, el material mostró alta deformación inducida, alta polarización y formación de enlaces Si-N, indicadores de una transición amorfa que podría producir un compuesto formado por granos o nanogranos de TiN embebidos en una matriz amorfa de Si-N. Mientras que al incluir 21 % de Si sustituyendo átomos de Titanio, se observó una distribución más estable, que puede producir diferentes fases del compuesto estequiométrico Ti1-xSixNy.

Palabras clave: teoría de funcionales de densidad; estructura cristalina; silicio; películas delgadas; recubrimiento.

1 Introduction

Titanium based structures has been studied extensively specially in hard coating applications, for example both nitrides (TiN) and carbides (TiC) or the combination called carbo-nitride ($TiCN$). These coatings are deposited on commercial substrates, because their excellent structural characteristics, mechanical and tribological properties [1],[2],[3],[4],[5], but high reactivity and low oxidation resistance limits their industrial applications in high temperatures environments (>500 °C). The addition of different atoms on the TiN lattice has shown to be a good method to improve hardness and oxidation resistance. This type of structures can be obtained by different deposition techniques like magnetron sputtering or cathodic arc [5],[6],[7],[8]. The hardness and oxidation resistance increases

when silicon is added to titanium nitride, due to the formation of TiN nano-crystalline/amorphous Si_3N_4 with nanocomposite structure (TiN nanocrystals embedded on a thin silicon nitride matrix), so that the dislocations in the nanocrystal cannot propagate across the silicon nitride over the grain boundary. Cracks formed on the amorphous matrix are anchored in the titanium nitride nanocrystals boundary, so high strength is necessary to produce deformation or failure, achieving hardness and young modulus up to 45 Gpa and 400 Gpa respectively [8],[9],[10]. Previously experimental and theoretical studies postulated that Ti-Si-N system stability is affected by Si atomic percent and the presence of mixed phases, reported as lateral compounds in the deposition process or by system inherent immiscibility such as Ti-$Si - N(O)$ and Ti/Si_3N_4 [11],[12],[13]. Experimentally $Ti_1 -_x Si_xN_y$ phase has been deposited using RF magnetron sputtering by F. Vaz et all [14], showing phase separation in the stoichiometric compound. They also reported an increase of mechanical properties and oxidation temperature with low Si percent [14]. The formation of binary phases indicates that is possible to obtain different configurations, resumed in four groups: 1) combination of different crystalline phases of the present elements, such as $TiSi_2$ or TiO_x and the formation of free Si, when is present over 15%. These materials have low mechanical and tribological properties; 2) the Si homogeneous solubility in the TiN FCC lattice to form the stoichiometric compound $Ti_1 -_x Si_xN_y$, with low content of silicon. This material has good tribological properties, but with high Si content it becomes unstable; 3) TiN nano-crystal structures in an amorphous Si_3N_4 matrix, with excellent properties and 4) a complete amorphous compound formed by an increase in crystal defects or decrease of the crystallite size below X ray diffraction detection limit, with high Si content [15],[16]. Theoretic studies about compound stability and behavior will give a full understanding on the formation of different coexisting phases in order to find the ideal deposition parameters for needed applications.

2 Experimental setup

In this paper the influence of the insertion of silicon atoms in the TiN lattice is studied, with the objective of determining the $Ti - Si - N$ formation mechanism. The composite simulations were performed using

Gaussian 03 software with 6-311G/6-31G databases, Single Point Energy method (SPE), with the unrestricted Hartree Fock approximation to find spin functions and electrostatic multipolar expansion. Local Density Approximation (LDA) energy functions were used for short range correlations and General Gradient Approximation (GGA) functions for long range. Dummy atoms were included in order to complete the periodicity of the crystalline lattice and avoid edge discontinuities in the total electrostatic potential. A $1x10^{-2}$ convergence values were achieved for the density functions and energy between 150 cycles [17],[18]. Computational time for all the simulations was superior to 12 hours. Obtained data was summarized by Mulliken charge distribution and electron total density mapped to the highest occupied molecular orbital (HOMO). For a simpler representation, 75% of the Van deer Walls radius was used. Experimental studies indicate that Si atoms insertion over 7% increases the probability of nano-composite formation composed of TiN nano-crystals in an amorphous SiN matrix ($nc-TiN/a-SiN$) [16], in order to overcome this experimental limit, 21% of Si atoms were inserted to the structures. Simulated structures corresponds to a face center cubic titanium nitride ($TiN{-}FCC$), tetragonal silicon nitride ($SiN{-}tet$), face center cubic silicon nitride ($SiN-FCC$), face center cubic titanium silicon nitride with 21% interstitial silicon ($Ti{-}Si{-}N{-}interstitial$) and face center cubic titanium silicon nitride with 21% substitutional silicon ($Ti{-}Si{-}N{-}substitutional$) (Figure 1). Table 1 shows the total energy obtained from the simulated structures.

Table 1: Total energy of the systems simulated.

Structure	Energy (Unrestricted Hartree Fock)
TiN-FCC	-1516.85016246 a.u.
Tetragonal SiN	-1698.78045000 a.u.
SiN-FCC	-4751.86989222 a.u.
Interstitial Ti-Si-N	-13306.26467050 a.u.
Substitutional Ti-Si-N	-2210.33348982 a.u.

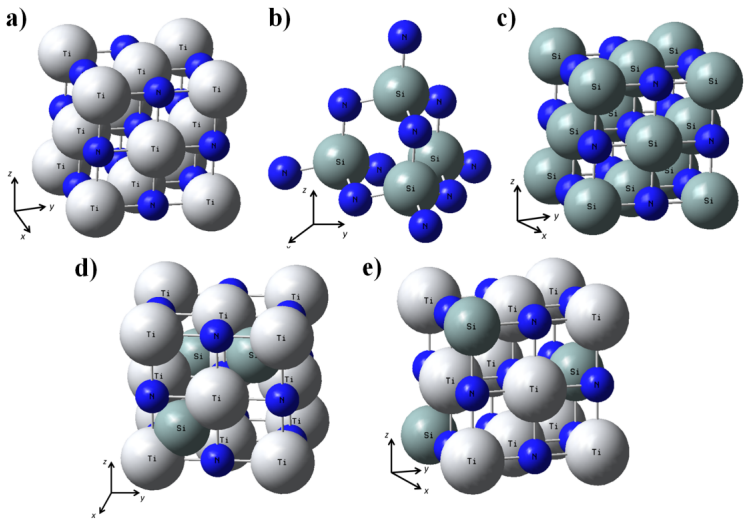

Figure 1: Simulated crystalline structures from: a) $TiN - FCC$, b) $SiN - tet$, c) $SiN - FCC$, d) $Ti - Si - N$ 21% interstitial Si and e) $Ti - Si - N$ 21% substitutional Si.

3 Results and discussion

Figure 1a shows TiN-FCC structure simulated, generating an interstitial nitride with lattice parameter of 0.424 nm; the array corresponds to a free stress structure reported by A. Devia et al [19]. This lattice parameter was used for all simulations in order to eliminate intrinsic variations caused by system sintering or deposition [2]. Figure 2a, shows Mulliken charges population analysis for $TiN - FCC$. The structure showed a neutral, stable behavior ($\sum q_1 = 0$) and spatial distribution depends on the element electronegativity. There is a high probability for other compounds to be formed, produced by chemical reactions after material sintering or thin film deposition, such as TiO_2 and TiO, Meanwhile nitrogen produces NH_2. However, NH_2 formation needs more energy, for that reason is expected that nitrogen stabilization is produced by association of N^+ ions to N_2 [13]. Figure 2b, shows total electron density of the TiN lattice mapped to the highest occupied molecular orbital (HOMO). The surface is continuous with polarizations produced by charge separation, as observed in the Figure

2a. This is agreement with the sp hybridization morphology that have been observed experimentally by X Ray Photoelectron Spectroscopy (XPS) [20]. The charge ranges from $-57.72x10^{-4}$ up to $57,72x10^{-4}$ a.u, showing symmetry, continuity and stability.

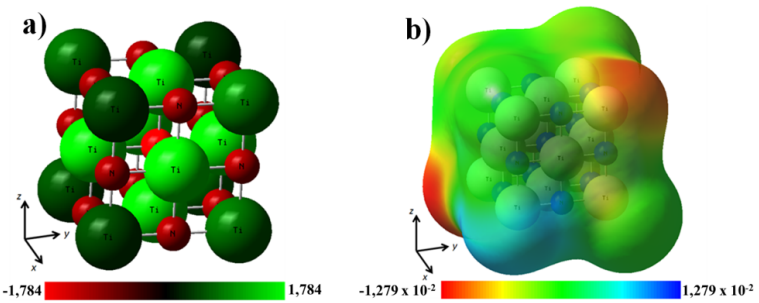

Figure 2: a) TiN-FCC Mulliken charges population analysis, charge range from -1.784 up to 1.784 a.u (atomic units). b) Electron total density mapped to the HOMO orbitals.

Initial discussion regarding the composition and crystalline structure of silicon nitride included the formation of two phases (α and β), both appearing to be hexagonal, with the c-axis dimension as principal difference between each other [21]. However, further research proved that silicon atoms were at the center of a tetrahedron, each nitrogen in trigonal and approximately planar coordination by three silicon (Figure 1b) [22]. Procedures to obtain the α and β structures of silicon nitride have been reported to be successful at high temperatures (above 1800K), due to the high intrinsic stress generated between the elements. Meanwhile the formation of tetragonal or amorphous silicon nitride is reported in low temperatures using high energy techniques, such as PVD and hybrid methods [23],[24].

Mulliken population analysis (Figure 3a) shows high polarization due to the high electronegativity of nitrogen atoms that attracts charges; meanwhile silicon atoms shoed reduced charge distributions. However the structure is stable ($\sum q_1 = 0$). High polarization of the atoms in the structure could indicate a polar bond between the elements; nevertheless orbital formed strongly indicates a covalent bond formation that has been confirmed both theoretically and experimentally [11],[13]. Figure 3b shows SiN-Tetragonal electron total density mapped to the HOMO orbitals. As

discussed above, an intrinsic polarization due to compound ceramic characteristics is observed. This phenomenon stabilizes with lattice expansion as studied by R.F. Zhang et al [11] and E.V. Shalaeva et al [13]. Charge range from $-1.05x10^{-2}$ to $1.05x10^{-2}$ a.u.

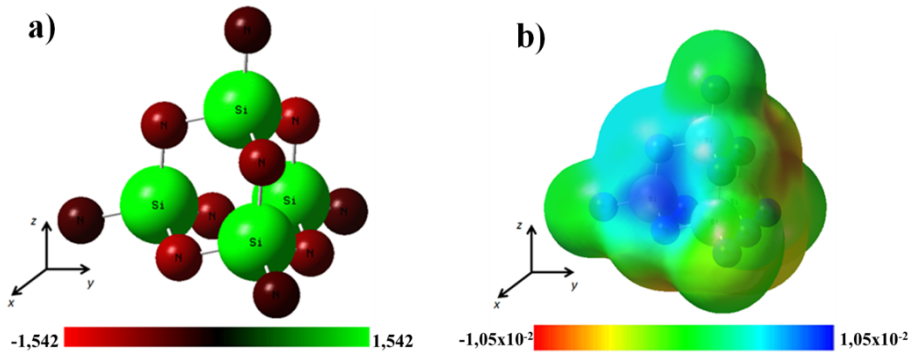

Figure 3: a) SiN- tetragonal Charge distribution, charge ranges from -1.542 to 1.542 a.u. b) Electron Total density mapped to the HOMO orbitals.

Face Center Cubic (FCC) silicon nitride has raised particular interest since the late 90's due to the theoretical prediction that the mechanical properties of several compounds with A3N4 stoichiometry (A: C, Si and B among others) may be comparable, of even higher to diamond. However Si3N4-FCC has shown to be metastable in air, returning to the α and β phase, oxidizing or becoming amorphous by a pressure increase [24].

$SiN - FCC$ simulated structure is shown in the Figure 1c. Mulliken charges population analysis (Figure 4a) showed a complete system polarization with high instability for the phase formation; however Mulliken charges sum is equal to cero [1]. High values in the change population analysis could indicate the absence of $Si - N$ bonds, tending to increase in energy with the number of atoms in the system as observed from Table 1, leading to instability for the 6 coordination number of the FCC structure. As the Mulliken population analysis explicitly depends on the basis set choice, the use of two different data bases reduced the uncertainty and comparable results were obtained [25]. $Si - Si$ or $N - N$ bond creation was discarded, indicating lateral compound formation after sintering; resulting in oxidation to SiO and SiO_2. The tetragonal SiN structure is predomi-

nant at the nano-composite interface. Control in the formation of lateral compounds will improve adherence between the matrix and the nano-grain [13]. Total electron density mapped to the HOMO orbitals (Figure 4b), shows polarization in the total density surface, this instability is related to absence of charge compensation on the center of the face. Charge ranges from $-1.564x10^{-2}$ to $1.564x10^{-2}$ a.u.

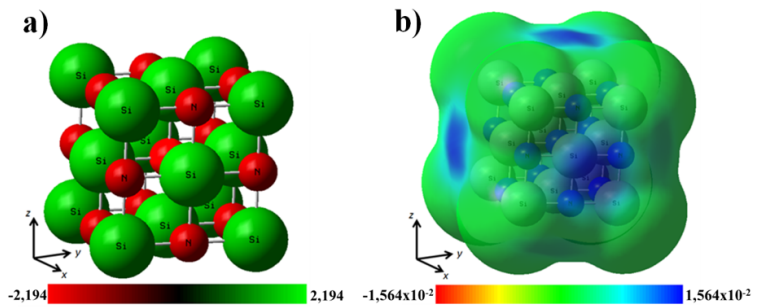

Figure 4: a) SiN- FCC Mulliken charges, range is from -2,194 up to 2,194 a.u. b) Electron total density mapped to the HOMO orbitals.

Figure 1d show $Ti-Si-N$ with 21% of interstitial silicon atoms located on the vectors $(1, \frac{1}{4}, \frac{1}{4})$â, $(\frac{1}{4}, \frac{3}{4}, \frac{1}{4})$â and $(\frac{1}{4}, \frac{3}{4}, \frac{3}{4})$â. The lattice parameter used (a=0.424 nm) correspond to the standard $\alpha - TiN$ in equilibrium [13],[16],[17]. Figure 5a shows the Mulliken population analysis of the simulated structure. Distribution shows low Charge separation between the elements, with an increase in the charge in Ti and N atoms. Titanium oxidation states indicate that there is a minimum probability of charge gain when an atom is a close neighbor with higher electronegativity, such as silicon. This observation could indicate an increase in probability of bond formation between $Si - Ti$ and $Si - N$. These bonds will lead to the amorphous phase of SiN with triple bond $Si - N$. While $Si - Ti$ bonds, indicates the formation of different phases $Ti - Si - N$, possibly$\beta - Ti - Si - N$, or a combination of α and β phases in meta-equilibrium [13]. The electron total density mapped to the HOMO orbitals (Figure 5b) shows low polarization on the opposite sites of the interstitial Si, which could confirm system instability. The polarizations observed on simulated TiN, that are due to sp hybridization, are nearly absent in the interstitial

$Ti - Si - N$ simulated. This indicates that lateral reactions have high probability, leading to the formation of different compounds. All this leads to the conclusion that interstitial silicon in the TiN lattice is unlikely (at least in these atomic sites), due to the formation of other compounds, by the absence of balance and the amount of energy needed to keep this particular system stability [15]. Charge ranges from $-1.221x10^{-2}$ to $1.221x10^{-2}$ a.u.

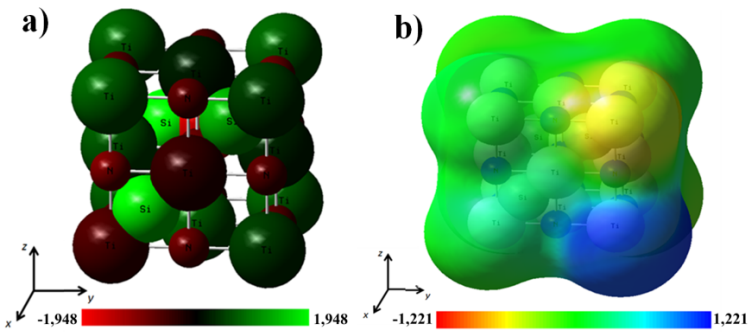

Figure 5: a) Mulliken population analysis, charge range is from -1.948 up to 1.948 a. u. b) Electron total density mapped to the HOMO orbitals.

Figure 1e shows $Ti - Si - N$ structure, with 21% of titanium atoms substituting silicon in the positions $(0, 0, 0)$, $(1, 0, 1)$ and $(\frac{1}{2}, 1, \frac{1}{2})$, with $\alpha - Ti_1 -_x Si_x N$ (FCC) crystalline structure and a=0.424 nm. The Mulliken charges distribution (Figure 6a), showed a stable system compared to interstitial silicon (Figure 5a). Charges are distributed according to elements electronegativity, nitrogen as high electronegative followed by silicon and titanium. Anomalies are not observed, as presented in the first structure and the same configuration is retained when charge symmetry is not forced between the elements. Creation and destruction of atomic bonds was observed and high state energy of $Ti - Si$ bond indicates the existence of different allotropic phases, $\beta - phase$ or an α/β combination. Some $Si - N$ and $Ti - N$ bonds disappear, probably due to unbalances between atoms, by electronegativity differences and absorption of charges by silicon atoms, which have oxidation states between -4 and $+4$ (without passing through zero)[11],[13],[15],[16]. Creation of double or triple bonds between the elements was not observed.

The electron total density (Figure 6b) is continuous. There is an improbable orbital overlap in the left front corner, generated by electrons in the titanium atom, due to the location of silicon in the vicinity. The same phenomenon is observed in all the titanium atoms near the silicon but to a lesser extent. In general, the structure is stable, but low formation probability is observed, due to $Ti - Si$ bond formation and $Ti - N$ and $Si - N$ bond destruction. It is possible that lateral structures are formed, as α ,β or γ (cubic) SiN and α and β TiN or other phases of the compound $(\alpha, \beta, \alpha - \beta Ti - Si - N)$ in meta-stable equilibrium [13]. Charge range from $-9,173x10^{-3}$ to $9,173x10^{-3}$ a.u.

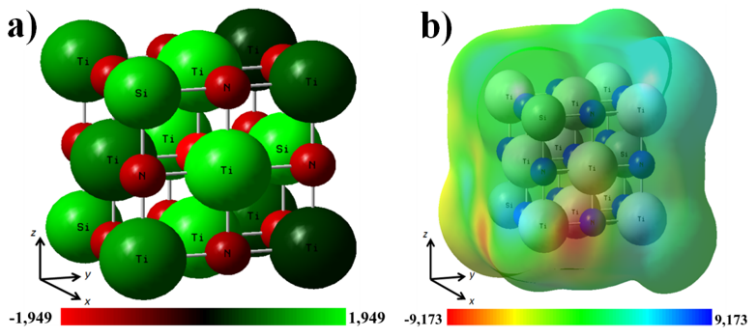

Figure 6: a) $Ti - Si - N$ 21% Si substitutional charges distribution. Charge range from $-1,949$ up to $1,949$ a.u. b) Electron total density mapped to the HOMO orbitals.

4 Conclusions

Computational methods allow determination, with a good range of certainty, of crystal structures behavior in terms of energy and stability. The use of DFT, to determine the influence of 21% Si in the $FCC - TiN$ showed that the $Ti - Si - N$ stoichiometric phase is at metastable equilibrium and there is high probability that the compound formed corresponds to an interstitial TiN alloy where Si atoms form Si_3N_4 as an amorphous matrix for TiN stable crystals. According to population analysis, there is a high probability of alternative compounds formation, due to nitrogen atoms migration and absence of $Si - N$ bonds with sp_2 hybridization, creating

another reaction path for the amorphous compound or other crystalline phases. Except for the separated compounds, there are anomalies in the total electron density, confirming the meta-equilibrium phase $Ti - Si - N$. The $FCC - SiN$ Mulliken charges population analysis showed a complete system polarization with high instability on the compound phase formation. This result may lead to the generation of amorphous silicon nitride in the nanocomposite material.

Acknowledgements

The authors wish to acknowledge the Universidad del Valle, for the support throughout the project number 2803.

References

[1] A. Muñoz, J. López, A. Ruden, D. Devia, V. Benavides, J. González, and A. Devia, "Descripción de Celdas FCC para Películas Delgadas de TiAlN por Métodos Computacionales," *Revista Colombiana de Física*, vol. 39, no. 1, pp. 139–142, 2007. 12, 17

[2] J. M. González, A. Ruden, A. Neira, F. Sequeda, and P. Leroux, "Influence of Substrate Temperature on Structure and Tribological Properties of TiAlNV," *Society of Vacuum Coaters*, vol. 51, pp. 666–672, 2008. 12, 15

[3] D. M. Devia, J. Restrepo, A. Ruden, J. M. González, F. Sequeda, and P. J. Arango, "The Tribological Characteristics of TiN, TiC, TiC/TiN Films Prepared by Reactive Pulsed Arc Evaporation Technique," *Society of Vacuum Coaters*, vol. 505, pp. 32–36, 2009. 12

[4] A. Murcia, A. Ruden, A. Neira, J. M. Gonzalez, I. Castro, S. Brulh, and F. Sequeda, "Tribological Properties of Duplex Coating Applied in Chrome Based Steel," *Society Vacuum Coaters*, vol. 505, pp. 37–43, 2009. 12

[5] M. F. Cano, J. S. Restrepo, A. Ruden, J. M. González, and F. Sequeda, "The Effect of Substrate Temperatures on Tribological Behavior of Ti-Al-N Coating Deposited by Magnetron Sputtering," *Rev. Society of Vacuum Coaters*, vol. 52, pp. 37–43, 2009. 12

[6] C.-L. Chang, W.-C. Chen, P.-C. Tsai, W.-Y. Ho, and D.-Y. Wang, "Characteristics and performance of TiSiN/TiAlN multilayers coating synthesized by cathodic arc plasma evaporation," *Surface and Coatings Technology*, vol. 202, no. 4, pp. 987–992, 2007. 12

[7] D. Devia, R. Ospina, V. Benavides, E. Restrepo, and A. Devia, "Study of TiN/BN bilayers produced by pulsed arc plasma," *Vacuum*, vol. 78, no. 1, pp. 67–71, 2005. 12

[8] S.-M. Yang, Y.-Y. Chang, D.-Y. Lin, D.-Y. Wang, and W. Wu, "Mechanical and tribological properties of multilayered TiSiN/CrN coatings synthesized by a cathodic arc deposition process," *Surface and Coatings Technology*, vol. 202, no. 10, pp. 2176–2181, 2008. 12, 13

[9] L. Rebouta, C. J. Tavares, R. Aimo, Z. Wang, K. Pischow, E. Alves, T. C. Rojas, and J. A. Odriozola, "Hard nanocomposite Ti–Si–N coatings prepared by DC reactive magnetron sputtering," *Surface and Coatings Technology*, vol. 133, pp. 234–239, 2000. 13

[10] Y. H. Cheng, T. Browne, B. Heckerman, and E. I. Meletis, "Mechanical and tribological properties of nanocomposite TiSiN coatings," *Surface and Coatings Technology*, vol. 204, no. 14, pp. 2123–2129, 2010. 13

[11] R. F. Zhang and S. Veprek, "Metastable phases and spinodal decomposition in Ti 1- x Al x N system studied by ab initio and thermodynamic modeling, a comparison with the TiN–Si 3 N 4 System," *Materials Science and Engineering: A*, vol. 448, no. 1, pp. 111–119, 2007. 13, 16, 17, 19

[12] M. Paulasto, F. J. J. Van Loo, and J. K. Kivilahti, "Stability and formation kinetics of TiN and silicides in the Ti/Si3N4 diffusion couple," *Le Journal de Physique IV*, vol. 3, no. C7, pp. C7—-1069, 1993. 13

[13] E. V. Shalaeva, S. V. Borisov, O. F. Denisov, and M. V. Kuznetsov, "Metastable phase diagram of Ti–Si–N (O) films (C Si< 30 at.%)," *Thin Solid Films*, vol. 339, no. 1, pp. 129–136, 1999. 13, 15, 16, 17, 18, 19, 20

[14] F. Vaz, L. Rebouta, P. Goudeau, J. Pacaud, H. Garem, J. P. Riviere, A. Cavaleiro, and E. Alves, "Characterisation of Ti 1- x Si x N y nanocomposite films," *Surface and Coatings Technology*, vol. 133, pp. 307–313, 2000. 13

[15] J. Houska, J. E. Klemberg-Sapieha, and L. Martinu, "Atomistic simulations of the characteristics of TiSiN nanocomposites of various compositions," *Surface and Coatings Technology*, vol. 203, no. 22, pp. 3348–3355, 2009. 13, 19

[16] F. Kauffmann, G. Dehm, V. Schier, A. Schattke, T. Beck, S. Lang, and E. Arzt, "Microstructural size effects on the hardness of nanocrystalline TiN/amorphous-SiN x coatings prepared by magnetron sputtering," *Thin Solid Films*, vol. 473, no. 1, pp. 114–122, 2005. 13, 14, 18, 19

[17] M. J. Frisch, G. W. Trucks, H. B. Schlegel, G. E. Scuseria, M. A. Robb, J. R. Cheeseman, J. A. Montgomery, Jr., T. Vreven, K. N. Kudin, J. C. Burant,

J. M. Millam, S. S. Iyengar, J. Tomasi, V. Barone, B. Mennucci, M. Cossi, G. Scalmani, N. Rega, G. A. Petersson, H. Nakatsuji, M. Hada, M. Ehara, K. Toyota, R. Fukuda, J. Hasegawa, M. Ishida, T. Nakajima, Y. Honda, O. Kitao, H. Nakai, M. Klene, X. Li, J. E. Knox, H. P. Hratchian, J. B. Cross, V. Bakken, C. Adamo, J. Jaramillo, R. Gomperts, R. E. Stratmann, O. Yazyev, A. J. Austin, R. Cammi, C. Pomelli, J. W. Ochterski, P. Y. Ayala, K. Morokuma, G. A. Voth, P. Salvador, J. J. Dannenberg, V. G. Zakrzewski, S. Dapprich, A. D. Daniels, M. C. Strain, O. Farkas, D. K. Malick, A. D. Rabuck, K. Raghavachari, J. B. Foresman, J. V. Ortiz, Q. Cui, A. G. Baboul, S. Clifford, J. Cioslowski, B. B. Stefanov, G. Liu, A. Liashenko, P. Piskorz, I. Komaromi, R. L. Martin, D. J. Fox, T. Keith, M. A. Al-Laham, C. Y. Peng, A. Nanayakkara, M. Challacombe, P. M. W. Gill, B. Johnson, W. Chen, M. W. Wong, C. Gonzalez, and J. A. Pople, "Gaussian. inc., wallingford, ct, 2005 - gaussian 03, revicion d. i," Gaussian, Inc., Wallingford, CT, 2004. 14, 18

[18] A. Frisch, M. Frisch, and G. Trucks, "Gaussian 03 User's reference," pp. 23–28, 2005. 14

[19] A. Devia, V. Benavides, E. Restrepo, D. F. Arias, and R. Ospina, "Influence substrate temperature on structural properties of TiN/TiC bilayers produced by pulsed arc techniques," *Vacuum*, vol. 81, no. 3, pp. 378–384, 2006. 15

[20] D. Jaeger and J. Patscheider, "A complete and self-consistent evaluation of XPS spectra of TiN," *Journal of Electron Spectroscopy and Related Phenomena*, vol. 185, no. 11, pp. 523–534, 2012. 16

[21] F. L. Riley, "Silicon nitride and related materials," *Journal of the American Ceramic Society*, vol. 83, no. 2, pp. 245–265, 2000. 16

[22] S. Wild, P. Grieveson, and K. H. Jack, "The crystal structure of alpha and beta silicon and germanium nitrides," *Special Ceramics*, vol. 5, pp. 385–395, 1972. 16

[23] A. Markwitz, H. Baumann, E. F. Krimmel, M. Rose, K. Bethge, P. Misaelides, and S. Logothetidis, "Nitrogen profiles of thin sputtered PVD silicon nitride films," *Vacuum*, vol. 44, no. 3, pp. 367–370, 1993. 16

[24] A. Zerr, G. Miehe, G. Serghiou, M. Schwarz, E. Kroke, R. Riedel, H. Fueß, P. Kroll, and R. Boehler, "Synthesis of cubic silicon nitride," *Nature*, vol. 400, no. 6742, pp. 340–342, 1999. 16, 17

[25] A. E. Reed, R. B. Weinstock, and F. Weinhold, "Natural population analysis," *The Journal of Chemical Physics*, vol. 83, no. 2, pp. 735–746, 1985. 17